Temperature Effects on Prism-Based Surface Plasmon Resonance Sensor *

LIN Kai-Qun(林开群), WEI Lai-Ming(魏来明), ZHANG Dou-Guo (张斗国), ZHENG Rong-Sheng(郑荣升), WANG Pei(王沛), LU Yong-Hua(鲁拥华)**, MING Hai(明海)***

Department of Physics, University of Science and Technology of China, Hefei 230026

(Received 4 September 2007)

We theoretically analyse the temperature effects on a surface plasmon resonance (SPR) sensor in Kretschmann configuration. The temperature effects include the thermo-optic effect and the dispersion of thermal-optic coefficient in the dielectric along with the thermal expansion effect, phonon–electron scattering and electron–electron scattering in the metal layer. We simulate the temperature dependence of the resonance position and the sensitivity of the SPR sensor under wavelength-interrogation and angular-interrogation mode of operation and the differences are pointed out in the two modes.

PACS: 07. 07. Df, 73. 20. Mf, 78. 66. Bz, 65. 40. − b

Surface plasmon resonance is a resonance phenomenon of surface charge density wave at the interface of a metal layer and a dielectric layer, which can be resonantly excited by TM-polarized light. The resonance condition depends on many parameters such as incident angle, wavelength, and the dielectric functions of the metal and dielectric. Surface plasmon can be optically excited by the method of attenuated total reflection (ATR) in the geometry of Kretschmann and Raether[1] or Otto.[2] SPR technology was first used for gas detection and biosensing by Nylander *et al.*[3] and Liedberg *et al*,[4,5] and now widely applied into gas detection, chemical sensing and biosensing.[6−9] Generally, SPR sensor has to be exposed to environments with varying temperature, the metal and dielectric properties will be modified by thermal-expansion effect, the phonon–electron scattering, the electron–electron scattering and thermo-optic effect. All these effects influence the performance of the SPR sensor. Chiang *et al.*[10,11] presented a model of the temperature effect on the sensitivity of a prism-based SPR sensor, the temperature dependence of the metal properties was considered, while the dielectric was not. Sharma *et al.*[12] studied the effect of temperature on the sensitivity and the signal-to-noise ratio (SNR) of a fibre SPR sensor. Both the temperature dependences of the dielectric and metal properties were considered, whereas the dispersion of the thermo-optic coefficient of the dielectric was not regarded. Further, the temperature dependence of the thermal expansion coefficient of the metal was not considered in the above models.

In this Letter, temperature effects, including the dependences of the thermal expansion coefficient of the metal and the dispersion of the thermo-optic coefficient of the prism along with the dependence of dielectric function of the prism and metal on temperature, are studied theoretically in the Kretschmann configuration. Two different operation modes of wavelength-interrogation and angular-interrogation mode are considered in our SPR sensor.

The device is in the Kretschmann geometry.[1] A silver film with thickness of d is coated on the bottom of prism; the analyte with refractive index of n_a is just on the surface of the silver film. The incident light of wavelength of $\boldsymbol{\lambda}$ is input into the prism. Surface plasmon at the interface between the silver film and the analyte is resonantly excited at a proper incident angle and at wavelength which depends on the permittivity of silver, prism and the analyte, also the thickness d of the silver film. In optics, the Kreschmann geometry is a typical three-layer system. Its refractivity can be calculated from the Fresnel equation

$$R_p = \left| \frac{r_{pm} + r_{ma}\exp(2ik_{mz}d)}{1 + r_{pm}r_{ma}\exp(2ik_{mz}d)} \right|^2, \tag{1}$$

$$r_{pm} = \frac{k_{pz}\varepsilon_m - k_{mz}\varepsilon_p}{k_{pz}\varepsilon_m + k_{mz}\varepsilon_p}, \tag{2}$$

$$r_{ma} = \frac{k_{mz}\varepsilon_a - k_{az}\varepsilon_m}{k_{mz}\varepsilon_a + k_{az}\varepsilon_m}, \tag{3}$$

$$k_{jz} = \left(\varepsilon_j \frac{\omega^2}{c^2} - k_x^2\right)^{1/2} \quad \text{for} \quad j = p, m, a,$$

$$k_x = \sqrt{\varepsilon_p}\frac{\omega}{c}\sin\theta. \tag{4}$$

Now let us realize how temperature contributes to the surface plasmon resonance and the reflectivity spectrum curve. Equation (1) exhibits that reflectivity signal of our device can be written in a formal function as $R_p(\varepsilon_a, \varepsilon_p, \varepsilon_m, d)$. It is clear that temperature effect can be understood from analysing the temperature-dependent properties of the metal film (ε_m, d) and prism (ε_p).

* Supported by the National Basic Research Programme of China under Grant No 2006cb302905, the National Science Foundation of China under Grant No 10474093, the Knowledge Innovation Project of Chinese Academy of Sciences under Grant No KJCX3.Syw.H02, and the National High-Technology Research and Development Programme of China under Grant No 2007AA06Z420.

** Email: yhlu@ustc.edu.cn

*** Email: minghai@ustc.edu.cn

©2007 Chinese Physical Society and IOP Publishing Ltd

The frequency-dependent dielectric function of silver is represented by the Drude model, i.e.

$$\varepsilon(\omega) = 1 - \frac{\omega_p^2}{\omega(\omega + i\omega_c)}, \tag{5}$$

where ω_p is the plasma frequency given by

$$\omega_p = \sqrt{\frac{4\pi N e^2}{m^*}} \tag{6}$$

with N and m^* represent the density and the effective mass of the conduction electrons, respectively. Hence ω_p at a given temperature owing to its thermal expansion effect can be calculated by using

$$\omega_p(T) = \omega_p(T_0) \exp\Big\{ -\frac{1}{2}\int_{T_0}^{T} \alpha_V(T) dT \Big\}, \tag{7}$$

where γ_0 is the room temperature (300 K) that acts as the reference temperature and $\alpha_V(T)$ is the volumetric thermal expansion coefficient of the metal which is varied with the temperature; $\alpha_V(T)$ is written as[13]

$$\alpha_V(T) = \frac{\gamma \cdot C_V(T)}{K}, \tag{8}$$

where γ is the Grüneisen constant, K is bulk modulus, and $C_V(T)$ is the specific heat at constant volume. According to the Debye approximation, $C_V(T)$ is written as

$$C_V(T) = 9Nk_B\Big(\frac{T}{T_D}\Big)^3 \int_0^{T_D/T} \frac{x^4 e^x}{(e^x - 1)^2} dx, \tag{9}$$

where T_D is the Debye temperature and k_B is Boltzmann's constant.

Figure 1(a) shows the volumetric thermal expansion coefficient of silver versus temperature. It is noted that when temperature is higher than the Debye temperature, the thermal expansion coefficient varies slightly with temperature; when temperature is lower than Debye temperature, it varies fast with temperature.

The collision frequency ω_c comes from phonon–electron scattering and electron–electron scattering $\omega_c = \omega_{ce} + \omega_{cp}$ with

$$\omega_{ce}(T) = \frac{1}{6}\pi^4 \frac{\Gamma\Delta}{hE_F}\Big[(k_B T)^2 + \Big(\frac{h\omega}{4\pi^2}\Big)^2\Big], \tag{10}$$

where Γ is a constant giving the average over the Fermi surface of the scattering probability, and Δ is the fractional Umklapp scattering,[14] ω_{cp} is described by the Holstein model of phonon–electron scattering,[15]

$$\omega_{cp}(T) = \omega_0\Big[\frac{2}{5} + 4\Big(\frac{T}{T_D}\Big)^5 \int_0^{T_D/T} \frac{z^4}{e^z - 1} dz\Big], \tag{11}$$

where ω_0 is a constant to each metal. As shown in Fig. 1(b), we can find that both the real part and the imaginary part of the metal-dielectric function for a silver layer increase with the increasing temperature.

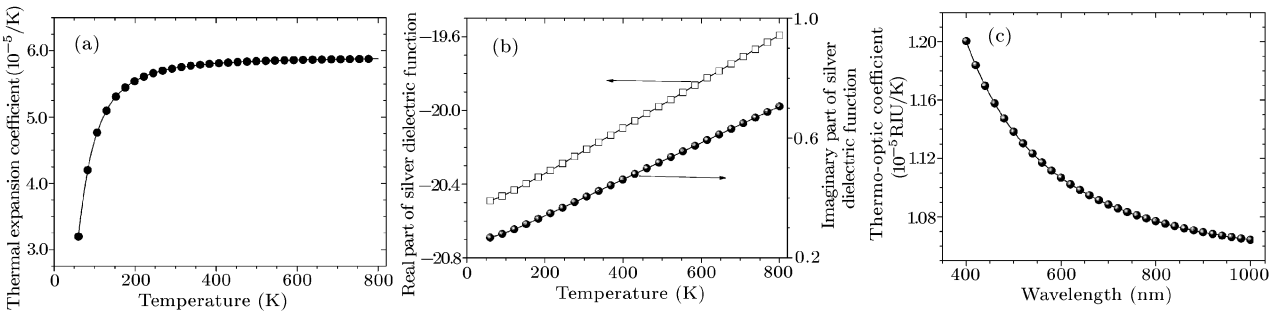

Fig. 1. (a) Volumetric thermal expansion coefficient of silver varies with temperature. (b) Variation of the real part and the imaginary part of the silver dielectric function with temperature at incident wavelength 632.8 nm. (c) Variation of thermo-optic coefficient of fused silica with wavelength. RIU: refractive index unit.

Another temperature effect for the metal film is the thermal expansion of the metal film makes a little correction on the film thickness d which is also an important parameter in the reflectivity (Eq. (1)). For a thin metal film, a corrected thermal-expansion coefficient $\alpha'_L(T)$ is employed for the expansion of the film thickness. The corresponding expression is[16]

$$\alpha'_L(T) = \alpha_L(T)\frac{1+\mu}{1-\mu}, \tag{12}$$

where μ is the Poisson number of metal, and $\alpha_L(T) = \frac{1}{3}\alpha_V(T)$ is the linear thermal expansion coefficient of the bulk material, $\alpha_V(T)$ is the volumetric expansion coefficient of the metal defined in Eq. (8). The film thickness is written as

$$d(T) = d_0 \exp\Big\{ \int_{T_0}^{T} \alpha'_L(T) dT \Big\}. \tag{13}$$

The values of the metal parameters used in our simulations are taken from Refs. [12,17] as follows: thickness at room temperature is $d_0 = 50$ nm, plasma frequency at room temperature is $\omega_p(T_0) = 1.3724 \times 10^{16}$ rad/s, Grüneisen's constant $\gamma = 2.45$, Bulk modulus $K = 101.0$ GPa, Debye temperature $T_D = 225$ K, $\omega_0 = 2.0347 \times 10^{13}$ rad/s, $\Gamma = 0.55$,$\Delta = 0.73$, Poisson number $\mu = 0.37$, Fermi energy $E_F = 5.48$ eV.

Now, let us come to the temperature effect for the prism. Here we consider a prism made of fused

silica. Using a thermo-optic coefficient dn/dT, the temperature-dependent refractive index can be expressed as

$$n_p(T) = n_p(T_0) + (T - T_0) \times \frac{dn}{dT}. \quad (14)$$

However, in the case of wavelength-interrogation mode, the situation is more complicated because of the dispersion of glass. Thus, both the refractive index and the thermal-optic coefficient are the functions of wavelength. It is known that the dispersion of fused silica is described by the Sellmeier equation

$$n_p(\lambda) = \sqrt{1 + \frac{A_1\lambda^2}{\lambda^2 - B_1^2} + \frac{A_2\lambda^2}{\lambda^2 - B_2^2} + \frac{A_3\lambda^2}{\lambda^2 - B_3^2}}, \quad (15)$$

where the coefficients A_1, A_2, A_3, B_1, B_2, and B_3 have certain numeric values and λ denotes the wavelength in units of μm. The above relation is valid for the wavelength range between 0.21 and 2.2 μm at room temperature. The thermo-optic coefficient for silica glass varies with wavelength is determined by[18]

$$2n_p(\lambda)\frac{dn_p}{dT}(\lambda) = GR + HR^2, \quad (16)$$

$$R = \lambda^2/(\lambda^2 - \lambda_{ig}^2), \quad (17)$$

where $n_p(\lambda)$ is the room-temperature refractive index, and λ_{ig} is the band gap wavelength of fused silica. The optical constants G and H are related to the thermal expansion coefficient and the temperature coefficient of the excitonic band gap, respectively. Taking the parameters[18,19] as follows: $A_1 = 0.6961663$, $A_2 = 0.4079426$, $A_3 = 0.8974794$, $B_1 = 0.0684043$, $B_2 = 0.1162414$, $B_3 = 9.896161$, $G = -1.6548 \times 10^{-6}$/K, $H = 31.7794 \times 10^{-6}$/K, $\lambda_{ig} = 0.109\,\mu$m, we calculate the dispersion of the thermal-optic coefficient of silica glass, dn/dT, as shown in Fig. 1(c). The dependence of thermal-optic coefficient on wavelength looks like a parabola, so it decreases fast in the period of short wavelength. In the wavelength range of our calculation (400 nm to 1 μm), thermal-optic coefficient decreases 11%.

Firstly, we simulate the temperature dependence of the resonance position and the sensitivity of the SPR sensor under the angular-interrogation mode of operation at fixed incident wavelength $\lambda = 632.8$ nm. The silver film thickness $d_0 = 50$ nm at room temperature 300 K, and the analyte is water, $n_a = 1.33$. Figure 2 gives the SPR curves of reflectivity depending on the incident angle at temperatures $T = 70$, 100, 200, 300, 400, 500, 600, 700, 800 K. It is noted that firstly the resonance angle shifts to a smaller value (from 73.039° to 72.427°) with the increasing temperature, secondly the SPR curve broadens with the increasing temperature.

To clarify the reason of resonant angle shift, we try to perform the simulation to separate the temperature effect from the metal film or thermo-optic effect of the prism. The results are shown in Fig. 3(a). The line group of 300 K, 400 K (B) and 500 K (B) is the serial SPR curves considering only the temperature effect of the metal film, it is noted that the resonant angle is larger at higher temperature (from 72.831° to 72. 941°); after adding into the thermo-optic effect of the prism, we have the SPR curves group of 300 K, 400 K (A) and 500 K (A), the resonant angle shifts to the other direction (from 72.831° to 72.666°). This means that the temperature effect of the metal film and the prism provide an opposite shift to the resonant position of the SPR curve.

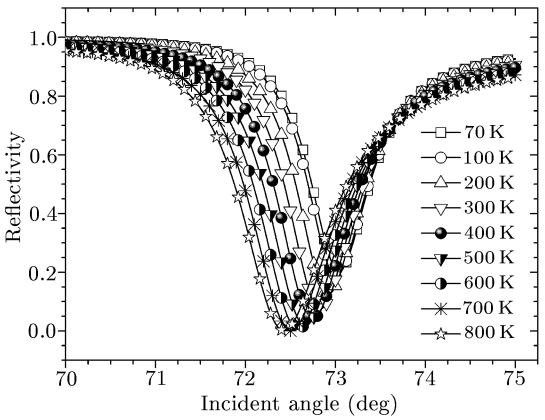

Fig. 2. Variation of reflectivity with incident angle at different temperatures.

Figure 3(b) shows how the resonance angle varies with the refractive index of the analyte (1.330–1.340) at different temperatures when the incident wavelength is fixed at 632.8 nm. The sensitivity in the angular-interrogation mode is defined as $S = d\theta_{\rm res}/dn_a$, and $\theta_{\rm res}$ is the resonant angle. As shown in Fig. 3(c), the sensitivity of the SPR sensor under angular interrogation mode shifts slightly to a smaller value with the increasing temperature, in the range of our calculation the sensitivity change is only 3%, which is neglectable.

The temperature effect is also analysed in the wavelength interrogation mode, in which light incident at a fixed angle ($\theta = 70°$), the reflectivity is as a function of wavelength. Other conditions such as the thickness of the metal film, the analyte material are the same with the angular interrogation mode. In Fig. 4(a), the SPR curves are calculated at temperatures $T = 70$, 100, 200, 300, 400, 500, 600, 700, 800 K. At first glance, it is similar to the case of angular interrogation mode (Fig. 2). However, further analysis exposes the difference. Figure 4(b) gives how the resonance wavelength varies with the refractive index of the analyte (1.330–1.335) at different temperatures when incident angle is fixed at 70°. It is found that the lines for different temperatures are not parallel as those in Fig. 3(b). If we draw out the sensitivity-temperature curve (Fig. 4(c)), the difference is more clear. Here the sensitivity

in the wavelength-interrogation mode is defined as $S = d\lambda_{\rm res}/dn_a$, and $\lambda_{\rm res}$ is the resonant wavelength. It is noted the sensitivity change in our calculation range is around 33%, the sensor is more sensitive at low temperature. Thus it can be concluded that temperature effect is more important in wavelength interrogation mode than that in angular interrogation mode. The possible reason is that the dispersion of thermo-optic coefficient and metal permittivity must be considered in wavelength interrogation mode.

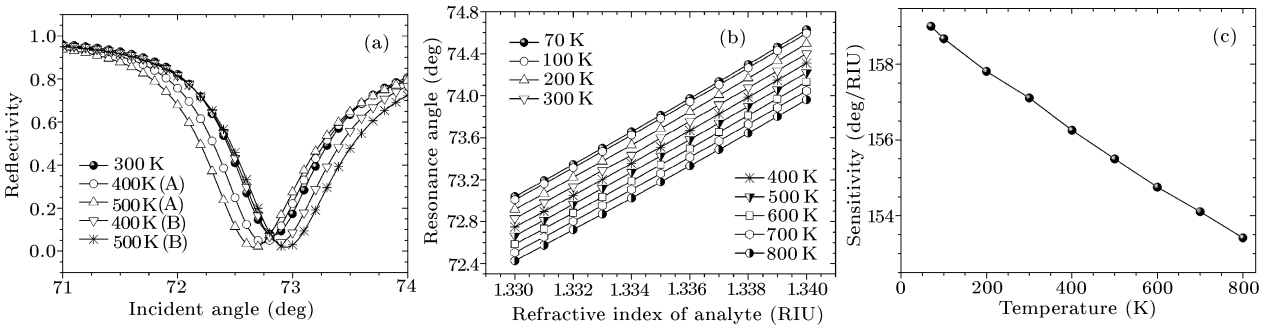

Fig. 3. (a) SPR curve between reflectivity and incident angle at 300 K ,400 K, 500 K with (A) and without (B) consideration of the change of refractive index of prism. (b) Variation of resonance angle with the refractive index of the analyte at different temperatures. (c) Variation of the sensitivity of the SPR sensor with temperature when $\lambda = 632.8$ nm and n_a ranges from 1.330 to 1.340. The sensitivity of the SPR sensor under angular interrogation mode is defined as the slope of the resonance angle over the refractive index of analyte.

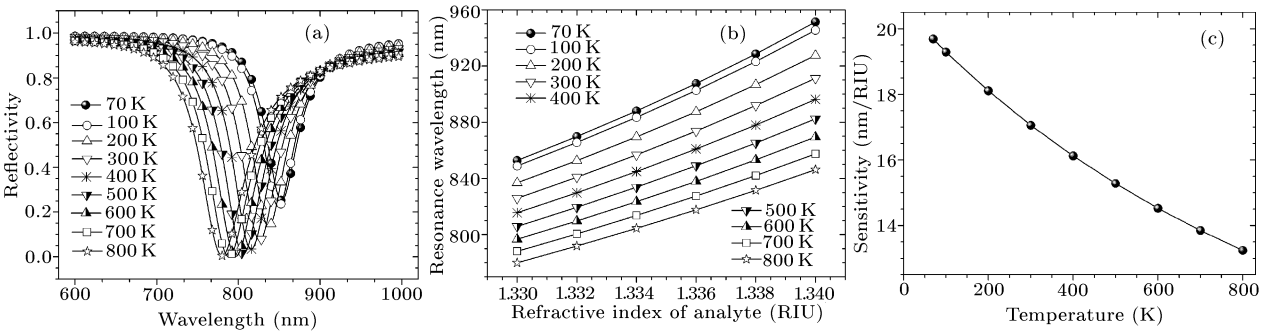

Fig. 4. (a) Variation of reflectivity with incident wavelength at different temperatures. (b) Variation of resonance wavelength with the refractive index of the analyte at different temperatures. (c) Variation of the sensitivity of the SPR sensor with the temperature when $\theta = 70^\circ$ and n_a ranges from 1.330 to 1.335, where it is different from Fig. 3(c) that the sensitivity of the SPR sensor under wavelength interrogation mode is defined as the slope of the resonance wavelength over the refractive index of analyte.

In summary, temperature effects on the sensitivity of the prism-based SPR sensor are analysed comprehensively. The SPR curve is shifted and broadened at high temperatures because properties of the metal layer and prism depend on temperature. The resonance position shifts to a smaller value and the sensitivity becomes lower with increasing temperature in both angular and wavelength interrogation modes, especially the sensitivity decreases more in wavelength interrogation. Our analysis may lead to better design and fabrication of SPR sensor against the temperature variation.

References

[1] Kretschmann E and Raether H 1968 *Z. Naturforsch.* **23** A 2135
[2] Otto A 1968 *Z. Physik* **216** 398
[3] Nylander C et al 1982 *Sensors Actuators* **3** 79
[4] Liedberg B et al 1983 *Sensors Actuators* **4** 299
[5] Liedberg B et al 1995 *Biosensors Bioelectron.* **10** i
[6] Homola J, Yee S S and Gauglitz G 1999 *Sensors Actuators* B **54** 3
[7] Lin H Y et al 2007 *Appl. Opt.* **46** 5
[8] Kim Y C et al 2005 *Opt. Lett.* **30** 17
[9] Mitsui K et al 2004 *Appl. Phys. Lett.* **85** 18
[10] Chiang H P et al 2001 *Opt. Commun.* **188** 283
[11] Chiang H P, Wang Y C and Leung P T 2003 *Thin Solid Films* **425** 135
[12] Sharma A K and Gupta B D 2006 *Appl. Opt.* **45** 1
[13] Huang K and Han LQ 1985 *Solid State Physics* (Beijing: Higher Education Press) p 122 (in Chinese)
[14] Lawrence W E1976 *Phys. Rev.* B **13** 5316
[15] Holstein T 1954 *Phys. Rev.* **96** 535
[16] Herminghaus S and Leiderer P 1990 *Appl. Phys.* A **51** 350
[17] Holzapfel W B et al 2001 *J. Phys. Chem. Ref. Data* **30** 2
[18] Gorachand Ghosh 1994 IEEE *Photon. Technol. Lett.* **6** 3
[19] Maiitson I H 1965 *J. Opt. Soc. Am.* **55** 1205